

Detecting desert dust events using IASI

Supervisors: Dr Elisa Carboni, Professor Roy Grainger

Candidate Number: 1006093

Project Number: AO23

Abstract

In this report the seasonal and inter-annual trends of desert dust in the atmosphere are studied using data from the Infrared Atmospheric Sounding Interferometer (IASI) satellite through measurements of aerosol optical depth (AOD) at a wavelength of 11 microns, over the years 2008-2015. Data from four different retrieval algorithms are used. In addition to studying the global trends, geographical locations considered are the Sahara (and desert dust transport across the Atlantic) and the UK. The Sahara is found to be the most prominent source of dust events in the world, which agrees with the current consensus. In all regions a very strong seasonal component is observed, with the largest AOD occurring in the summer and minimum in the winter. A multi-year trend is also studied, both regionally and worldwide. The results indicate that there has been no statistically significant change in the total volume of desert dust events in the time period considered. Dust transport across the Atlantic is studied in closer detail. According to the Université Libre de Bruxelles (ULB) retrieval the Sahara experiences a mean AOD of 0.082 in June and 0.016 in January. The corresponding values are 0.027 and 0.002 for the Amazon. An estimate of the proportion of dust reaching the Amazon from the Sahara is calculated to be 54%, using the Infrared Mineral Aerosol Retrieval Scheme (IMARS). The amount of dust in the Sahara region being studied (at the time of maximum AOD, June, and averaged over all years) is calculated to be 7.7×10^8 kg.

1 Introduction

Desert dust is an aerosol, which are suspended solid/liquid particles in the atmosphere that typically remain in the atmosphere of the order of one week. It plays an important role in the atmosphere for several reasons. Dust has a large effect on the radiative balance of the atmosphere by absorbing, reflecting and scattering both incom-

ing shortwave radiation and outgoing longwave radiation (although it is still unclear whether it has a net cooling or warming effect) (Slingo et al. 2006). It can also indirectly affect the atmospheric state by acting as cloud condensation nuclei (Bangert et al. 2012). Aerosols are one of the primary causes of uncertainty in climate models (due to cloud-aerosol interactions) (Schwartz and Andreae 1996). A better understanding of the location and magnitude of desert dust events could prove to be useful when improving global climate models.

Dust transport from the Sahara also fertilises the ecosystems of the Atlantic ocean (Kaufman et al. 2005) and the Amazon (Moran-Zuloaga et al. 2018). Dust storms can cause severe health problems in urbanised areas (primarily respiratory problems) (De Longueville et al. 2012), and cause millions of dollars worth of damage to the agricultural industry through damaging crops and livestock. These effects have the potential to cause harm far away from dry-lands due to the large distance over which dust can be transported in a relatively short amount of time. It has also been shown that anthropogenic climate change, causing desertification, and soil erosion due to unsustainable agricultural practices could result in increased levels of desert dust (Li et al. 2007); which in turn could result in even more severe local climate disturbance due to the effects of dust on radiative balance. This means it will be interesting to study the measurement period which is available (IASI was launched in 2006 but continuous data is only currently available for the years 2008-2015), to see if there has been any statistically significant increase in desert dust events, which could be linked to human activity. A lack of significant change in desert dust events would be insufficient to rule out a long term trend, as eight years of data is not a large timescale.

Studying the seasonality of desert dust is also important. A periodic behaviour will give insight into the mechanisms producing the dust (e.g. does a time of year with stronger winds result in more dust being blown into the atmosphere?) and could also allow other periodic phenomena in the atmosphere to be linked to desert dust (e.g.

does more rainfall at certain times of year in certain regions correspond to more/less desert dust, or is there only a very weak correlation?). Dust produced by the Saharan desert will be the main focus as this is by far the most prominent source of dust worldwide (>50% of global dust, Huneus et al. 2011). There has been previous research on the detection of desert dust events. Saharan dust was studied (Marticorena and Bergametti 1996) over a two year period from 1991-1992, with monthly mean production of approximately 600Mt. Their results showed desert dust peaking in the spring, with a small overall difference of (12%) in the total dust measured between 1991 and 1992.

In this report, a brief overview of the retrieval algorithms used (the physics behind them) will be given, and their relative advantages/disadvantages will be commented upon. In the results section these outputs will be looked at, and the extent to which the results can be relied upon for detecting desert dust events will be discussed. Although the transport of desert dust across the North Tropical Atlantic is a well known phenomenon, there has been no research involving an attempt to quantify the proportion of dust reaching the Amazon from the Sahara. An estimation of both the proportion and mass of dust reaching the Amazon will be calculated. Finally, all of the results will be drawn upon and an assessment of what was achieved by this project will be discussed, as well as suggesting potential improvements and modifications for future research in this area.

2 Method

The primary output of the retrieval algorithms is aerosol optical depth (AOD) at a wavelength of 11 microns. Optical depth is defined as (Andrews 2010):

$$\tau = \ln\left(\frac{\phi_e^i}{\phi_e^t}\right) = \int_z^\infty k_v(z')\rho_a(z')dz' \quad (1)$$

where ϕ_e^i is the radiative flux incident on the material, ϕ_e^t is the radiative flux transmitted by the material, k_v is the extinction coefficient, ρ_a is the

density of the absorbing/scattering material, and integrating from the top of atmosphere ($z = \infty$) to the surface. If a region is considered to be optically thin (optical depth of far less than one, which is the case for the results) the aerosols can also be assumed to simply form a horizontal layer in the atmosphere, as it can be assumed that the particles are sufficiently spread apart that very few will overlap with the same path of a light beam in the line of sight from the satellite. Furthermore, if scattering is assumed to be the dominant radiative effect, and the particles are assumed to be spherical (such that they have a cross section in the shape of a circle), the aerosol optical depth can be defined as:

$$\tau = Q_{scat}N\pi r^2 \quad (2)$$

Where Q_{scat} is the scattering coefficient, N is the number of particles per unit area, and r is the radius of the particles. Strictly speaking equation (2) should be an integral over the size distribution, but the result above is valid assuming all particles have the same radius. From equation (2) it can be seen that AOD is directly proportional to N , and therefore also directly proportional to the mass of scattering material in the region being considering, assuming all particles have the same radius.

To get a value for the mean AOD for a region, rectangular boxes between certain values of latitude and longitude are considered. Values for AOD are given at each integer value of latitude and longitude (monthly mean data). For example, if a box between 5° and 30° latitude and -30° and -5° longitude is being studied, there will be $25 \times 25 = 625$ data points. Taking the mean of these points (and filtering out points for which there are no measurements, for which the AOD is set to -999), a mean AOD can be calculated. The mean value does, however, include values where AOD is zero i.e. where the retrieval algorithm has produced an output but has determined there is no aerosol. With this information different trends can be studied. Firstly, the whole time series can be plotted. A mean seasonal AOD can also be plotted, which reveals if there is a periodic seasonal behaviour. A seasonally adjusted time series can also be plotted (i.e.

for each monthly data point plot that month’s mean over all years subtracted from the month in question), thus removing any seasonal variation from the multi-year trend and revealing any net increase in desert dust events over the time period considered.

2.1 Data/IASI

The data used for this project comes from IASI onboard the METOP satellite. Data is available for the years 2008-2015. Level 3 data (NetCDF) files (monthly gridded $1^\circ \times 1^\circ$ datasets) are used. Data from IASI was used for this project as it measures in the infrared, and desert dust shows strong optical activity in the infrared because of a strong resonance band at 11 microns (Klüser et al. 2016), meaning it can be distinguished from other species. While dust has been extensively studied in the visible region of the EM spectrum, less has been done in the infrared.

2.2 Retrieval Algorithms

According to Kinne et al. 2017: “Considering the most recent versions, the Université Libre de Bruxelles retrieval (ULB) maintained its top skill status. Otherwise quantitatively only the Laboratoire de Météorologie Dynamique retrieval (LMD) can be recommended.” Therefore, despite always using data from all four retrievals most trust is placed upon the results from the ULB retrieval. The ULB algorithm does not retrieve the aerosol radius and thus in order to make an estimate of the mass of the dust the other retrievals are required. Furthermore, although the other algorithms systematically overestimate AOD compared to the ULB retrieval they still produce the same seasonal variation as the ULB retrieval meaning they can be relied upon to pick up general patterns in the AOD. All of the algorithms also underestimate the AOD over the Sahara (Kinne et al. 2017) but are more accurate over ocean (as surface emissivity values are far more accurate over the ocean than land) so when measuring the AOD in the Sahara an area just to the west of the African north-west coast is actually used as a proxy for the Sahara.

Throughout this report all four retrievals are plotted, the following table shows the colour in which each retrieval is plotted:

ULB	Black
MAPIR	Blue
IMARS	Green
LMD	Red

2.2.1 ULB IASI Dust Retrieval

The following information is based upon a report by Clarisse 2017. The algorithm uses a neural network, and the neural network is trained using a forward model from Clarisse et al. 2010. The retrieval assumes the following input parameters (i.e. information that doesn’t come from IASI but has to be taken from other sources): surface elevation, surface emissivity (very good data available for ocean emissivity, less so overland), aerosol size distribution (lognormal distribution with geometric mean radius of 0.5 and geometric standard deviation of 2), refractive index, and altitude.

2.2.2 IASI LMD Dust Retrieval

The following information is based upon a report by Capelle and Chédin 2017. The retrieval uses a forward radiative transfer model, and has input parameters: atmospheric temperature profile, water vapour profile, surface temperature, surface pressure, and surface emissivity. For a size distribution it uses that of the AERONET (ground based aerosol detection) database giving a mean radius of $2 \mu\text{m}$ and a standard deviation of $0.65 \mu\text{m}$. Simulated look-up tables are then used to calculate the AOD and the aerosol altitude.

2.2.3 MAPIR Dust Retrieval

The following information is based upon a report by Vandembussche 2017. It uses the LIDORT forward model, and uses an optimal estimation iterative method. This algorithm retrieves both the AOD and surface temperature. It assumes a mean radius of $0.6 \mu\text{m}$, and a geometric standard deviation of 2. Also mentioned in the report

is the fact that there are no reliable databases for daytime desert surface temperature, causing particular problems for this retrieval which is extremely sensitive to this parameter.

2.2.4 IMARS Dust Retrieval

The following information is based upon a report by Klüser 2017. This is the only algorithm that currently retrieves, in limited cases, a value for the mean effective radius of the dust under consideration. It also uses forward simulations and stores the outputs in look-up-tables, in order to reduce computational cost.

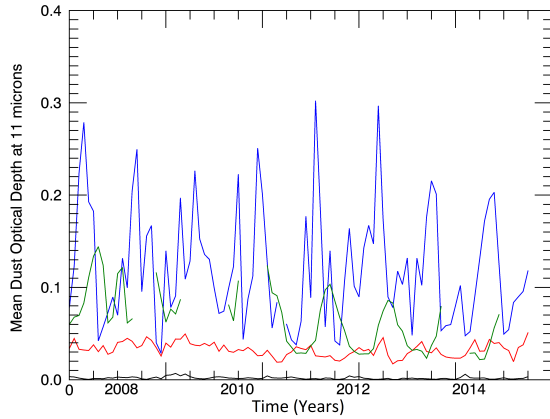


Figure 1: Plot showing AOD above the UK (Latitude range: $[50,58]$, Longitude Range: $[-3,7]$). The ULB algorithm predicts an AOD very close to zero for the entirety of the UK. Desert dust transport to the UK is not a well researched area, although there is research suggesting there is a small amount of transport to central Europe (Israelevich et al. 2012).

3 Results

To decide upon the regions to study the world mapping of AOD for the entire time series was studied (Figure 5, next page), to see which regions displayed high levels of AOD.

3.1 Sahara-Amazon Dust Transport

As can be seen in the figures below, where the entire time series of the AOD has been plotted for the 3 regions shown, there is a clear reduction in AOD across the Atlantic. However, assuming the primary source of dust on the west of the Atlantic comes from the Sahara, it can be seen that there is nevertheless a significant proportion being transported.

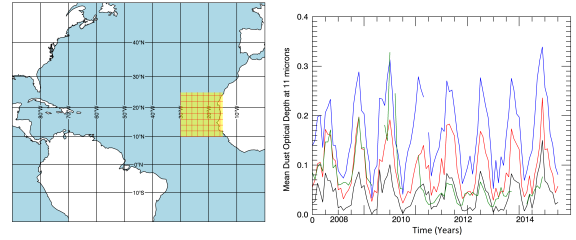


Figure 2: Sahara AOD. Latitude range: $[10,25]$. Longitude range: $[-30,-15]$.

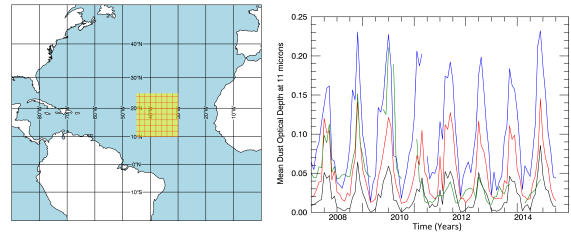


Figure 3: Atlantic AOD. Latitude range: $[10,25]$. Longitude range: $[-45,-30]$

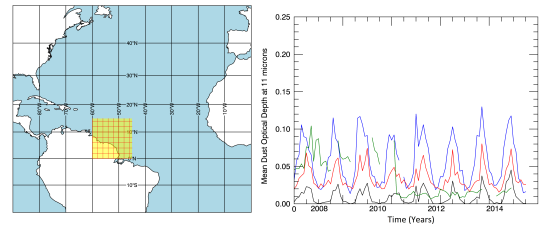


Figure 4: Amazon AOD. Latitude range: $[0,15]$. Longitude range: $[-60,-45]$

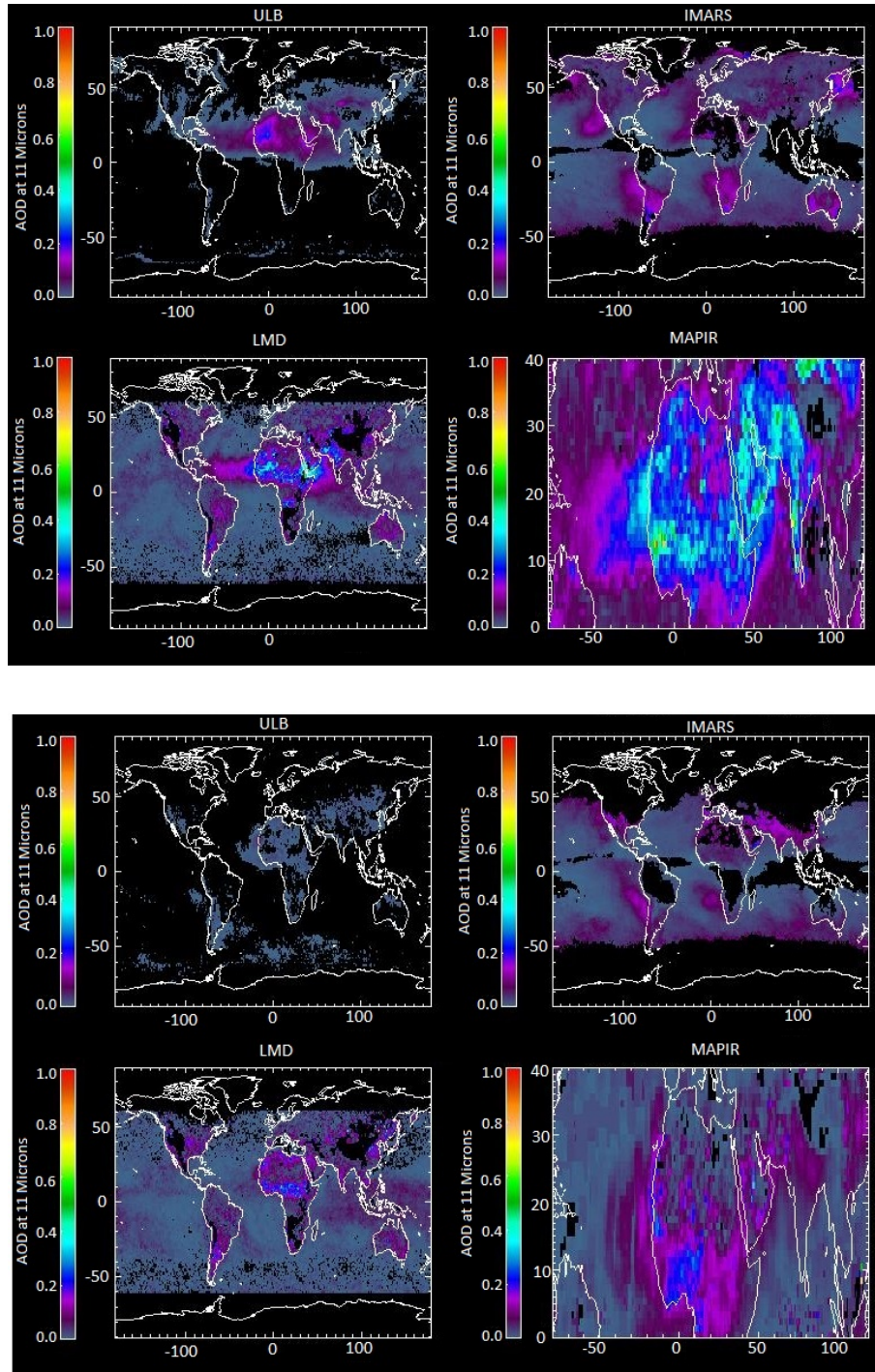


Figure 5: Graphic showing the AOD plots for all 4 algorithms for June 2013 (top) and December 2013 (bottom). It can be seen that the average AOD is far lower in December compared to June. The ULB algorithm (top left) provides the most accurate data. It is clear that the other three algorithms measure larger AODs, particularly MAPIR. Dust transport can be seen across the North tropical Atlantic. The MAPIR retrieval has been plotted over a smaller region in this case to show clearly the higher magnitude of AOD in Africa. Note: both non-measurement and a zero measurement of AOD are shown as black.

3.2 Seasonality

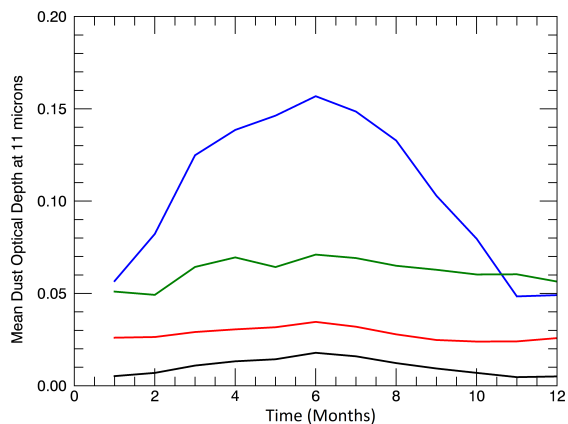


Figure 6: Plot showing the global seasonal variation of AOD.

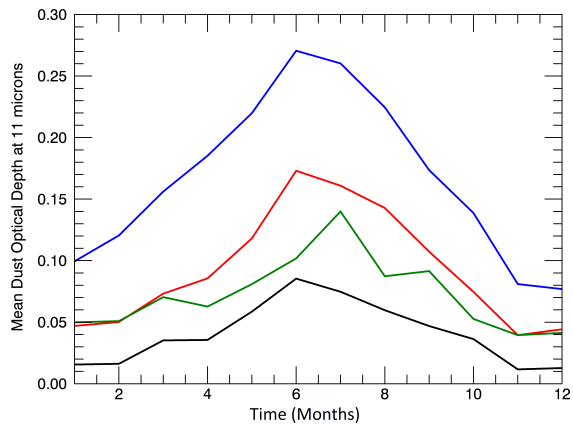


Figure 7: Plot showing the seasonal variation of the Sahara optical depth.

Figure 6 and figure 7 show that desert dust has a very strong seasonal component, it appears to be by far the largest factor in the determination of AOD. For the worldwide results, the LMD and IMARS retrievals have less pronounced seasonal variation than smaller regions (such as the Sahara) studied but the ULB and MAPIR retrieval still reveal a seasonality.

3.3 Multi-year trend

Figure 8 shows that whilst there is some variation for the MAPIR and IMARS retrieval in the global plot it can be seen that both the ULB and LMD retrieval show very little variation over the time period. This indicates that on a global scale there has been little change in the number of desert dust events. The Sahara (figure 9) shows greater fluctuations than the global plot, showing that there is some variation year on year in how much dust is produced by the Sahara. It doesn't reveal any long term net increase/decrease.

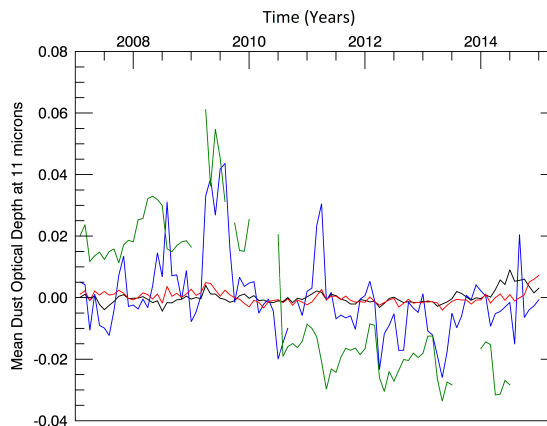


Figure 8: Plot showing the global seasonally adjusted AOD.

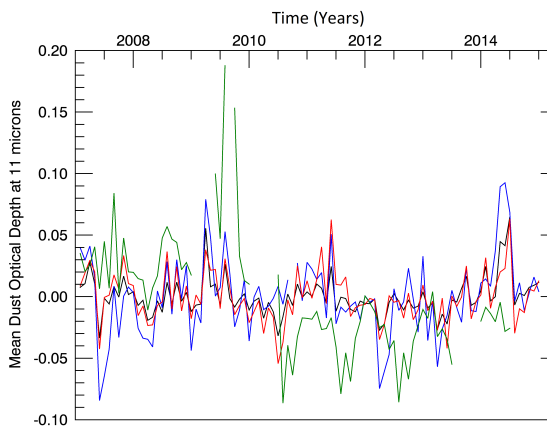


Figure 9: Plot showing the Sahara seasonally adjusted AOD.

3.4 Estimation of Mass Transport across Atlantic

Equation (2) was used to assume AOD is proportional to the mass of dust in the box being considered. Then simply taking the ratio of AOD in the Sahara and AOD in the Amazon (same regions as shown in map above) an estimate of the proportion of dust getting across the Atlantic can be calculated. Taking the mean across the entire IMARS data set:

$$\frac{\langle AOD_{Amazon} \rangle}{\langle AOD_{Sahara} \rangle} = 0.54 \quad (3)$$

The IMARS retrieval algorithm produced a

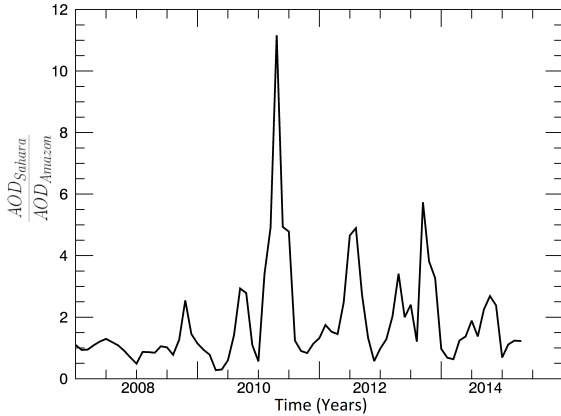


Figure 10: Plot showing the ratio of AOD in Sahara to AOD in Amazon

value for mean effective radius and mass density per m^2 , so data from this retrieval algorithm is used for the following calculations. As mentioned in section 2.2, this is one of the less accurate retrievals and therefore there is a large degree of uncertainty in these calculations. Even though this algorithm did retrieve these values, it only retrieved them for a small percentage of all AOD measurements; this means when considering a small grid box there would be very few, if any, measurements of mean effective radius or mass density per m^2 . Therefore, the distribution of radii and mass density per m^2 across the whole world was studied and it was seen that it was fairly constant between different areas. This

means (out of practicality) it would be a reasonable approximation to say that the mean radius of the particles in one region is approximately the same as the mean radius of the particles all over the world ($\langle r \rangle = 2.04 \times 10^{-5}$). Then the AOD in the region will determine the total mass of dust in that region. In places where there is no AOD measurement or AOD equals zero, the radius is not included in the value for the mean radius. Rearranging (2), gives:

$$N = \frac{\tau}{Q_{scat} \pi r^2} \quad (4)$$

The scattering coefficient can be found using Mie scattering theory. Using a refractive index of 1.55 for dust in the infrared (Petzold et al. 2009), gives a value of approximately 2. Calculating a value for N, then calculating the area of a grid box using:

$$A = \frac{\pi}{180} R^2 | \sin(lat_1) - \sin(lat_2) || lon_1 - lon_2 | \quad (5)$$

the total number of dust particles in a grid box can be calculated. The mean density of dust particles from the Sahara is 2.6 gm^{-3} (Wagner et al. 2009). Then, assuming each particle is a sphere the total mass in a grid box can be calculated. For an AOD of 0.172 (which is the mean AOD for the IMARS retrieval for June in the Sahara averaged over all years) this gives a value of $7.7 \times 10^8 \text{ kg}$. Equivalently, the amount of dust in the atmosphere above the Amazon in June (mean over all years) can be calculated as $4.2 \times 10^8 \text{ kg}$.

The retrieval also gives a value for mass density per m^2 . AOD is not needed to calculate the value for the mass in a box using this value, it can be calculated by simply multiplying the mass density per m^2 by the area being considered to calculate a total mass. This value will be independent of the region we are looking at, it is nevertheless a useful number to calculate as by the assumptions given above it should give a similar order of magnitude to the value of AOD calculated using equation (2). The mean value calculated using this method gives $5.4 \times 10^8 \text{ kg}$. This value is 30% more than the one calculated, but given that it is of the same order of magnitude this indicates that the method itself is

valid. This doesn't mean the answer is close to the "true" value, it just means that both methods have the same systematic biases.

The methods described have probably overestimated the proportion of dust reaching the Amazon. The IMARS retrieval predicts that 54% from the Sahara region considered reaches the Amazon region (having assumed that there are no sources of desert dust in the Amazon itself or being transported to the Amazon from another region, when this is almost certainly not entirely true). However, by looking at the plots from section 3.1 it can be seen that the ULB retrieval predicts a smaller amount of transport. The ULB retrieval gives a mean AOD of 0.082 for June in the Sahara and a mean AOD of 0.027 for June in the Amazon. This would give a percentage transport of only 32%.

3.5 Area Variability

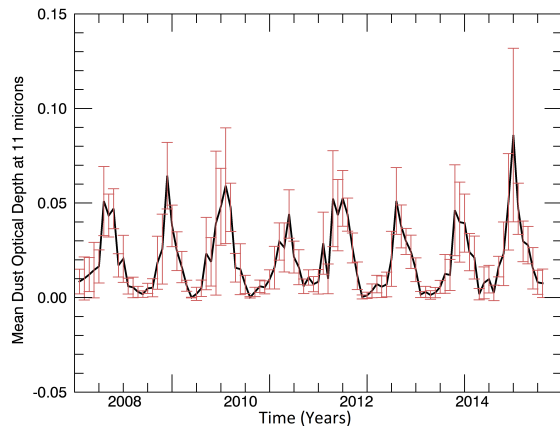


Figure 11: A plot of the ULB retrieval in the Sahara with standard deviation included for each month. For the sake of clarity only one retrieval is plotted, as they all show the same pattern.

The plot above shows the ULB time series with the standard deviation of all the points in the box being considered. Larger AOD values also have larger standard deviation, which is what is expected to happen. For the ULB retrieval each grid box would always have some measure-

ments of zero AOD. If the other data points had large values of AOD (as in the summer), this would result in a larger variance/standard deviation whereas if the other values of AOD were relatively low (as in winter) this would result in a smaller variance between the points.

4 Conclusion

In this report, IASI data has been used to study the trends in desert dust, specifically focusing on the Sahara and dust transport across the Atlantic to the Amazon. The results revealed a strong seasonal trend, with all regions measured undergoing predictable oscillation with a maximum AOD in the summer and minimum AOD in the winter.

Looking at the seasonally adjusted multi-year data revealed that total AOD produced per year has remained approximately constant, whilst the IMARS and MAPIR retrieval did fluctuate, the LMD and ULB retrievals, which are the more reliable ones, remained fairly constant throughout.

A constant AOD over these years can be used to infer that total desert dust events have not increased dramatically in the years 2008-2015, suggesting that land erosion has had little effect on desert dust in the atmosphere or that the magnitude of the dust produced due to anthropogenic causes is small compared to that produced 'naturally'. However, this is a relatively short period of time. In reality anthropogenic effects could be having an effect, but it will only be observable over a much larger time frame. An estimate of the proportion of mass being transported across the Atlantic gave a value of 0.54, although this is likely to be a large over-estimate.

To go further with this research, a more thorough statistical analysis could be performed on the data. Some of the retrieval algorithms used are still in development, giving scope to go further with the ideas discussed. If more parameters such as mean effective radius were outputted from the ULB or LMD retrieval this would allow a more accurate estimation of the mass of desert dust in the atmosphere. Furthermore, if the data set for radii was larger than that which was used,

a radius distribution could be used, rather than just using a mean radius. Also, the half-life of dust in the atmosphere is strongly dependent on desert dust size. Larger dust particles experience far more friction as a proportion of their mass, so fall much faster. By integrating this information into the calculation a better estimate of the dust transport could be made.

5 Bibliography

References

- Andrews, David G. (2010). *An Introduction to Atmospheric Physics*. 2nd ed. Cambridge University Press. DOI: 10 . 1017 / CB09780511800788.
- Bangert, M. et al. (2012). “Saharan dust event impacts on cloud formation and radiation over Western Europe”. In: *Atmospheric Chemistry and Physics* 12.9, pp. 4045–4063. DOI: 10 . 5194 / acp - 12 - 4045 - 2012. URL: <https://www.atmos-chem-phys.net/12/4045/2012/>.
- Capelle, Virginie and Alain Chédin (2017). “ESA Climate Change Initiative *aerosolcci2* Dust properties retrieval Algorithm Theoretical Basis Document (ATBD) Version 2.1”. In: URL: http://cci.esa.int/sites/default/files/Aerosol_cci2_ATBD_IASI_LMD_v2.1.pdf.
- Clarisse, Lieven (2017). “ESA Climate Change Initiative *aerosolcci2* ULB IASI Dust Retrieval Algorithm Theoretical Basis Document (ATBD) Version 1.7t”. In: URL: http://cci.esa.int/sites/default/files/Aerosol_cci2_ATBD_IASI_ULB_v1.7.pdf.
- Clarisse, Lieven et al. (2010). “Retrieving radius, concentration, optical depth, and mass of different types of aerosols from high-resolution infrared nadir spectra”. In: *Appl. Opt.* 49.19, pp. 3713–3722. DOI: 10.1364/AO.49.003713. URL: <http://ao.osa.org/abstract.cfm?URI=ao-49-19-3713>.
- De Longueville, Florence et al. (2012). “Desert dust impacts on human health: An alarming worldwide reality and a need for studies in West Africa”. In: *International journal of biometeorology* 57. DOI: 10 . 1007 / s00484 - 012 - 0541 - y.
- Huneeus, N. et al. (2011). “Global dust model intercomparison in AeroCom phase I”. In: *Atmospheric Chemistry and Physics* 11.15, pp. 7781–7816. DOI: 10.5194/acp-11-7781-2011. URL: <https://www.atmos-chem-phys.net/11/7781/2011/>.
- Israelevich, P. et al. (2012). “Predominant transport paths of Saharan dust over the Mediterranean Sea to Europe”. In: *Journal of Geophysical Research: Atmospheres* 117.D2. DOI: 10 . 1029 / 2011JD016482. eprint: <https://agupubs.onlinelibrary.wiley.com/doi/pdf/10.1029/2011JD016482>. URL: <https://agupubs.onlinelibrary.wiley.com/doi/abs/10.1029/2011JD016482>.
- Kaufman, Y. J. et al. (2005). “Dust transport and deposition observed from the Terra-Moderate Resolution Imaging Spectroradiometer (MODIS) spacecraft over the Atlantic Ocean”. In: *Journal of Geophysical Research: Atmospheres* 110.D10. DOI: 10.1029/2003JD004436. eprint: <https://agupubs.onlinelibrary.wiley.com/doi/pdf/10.1029/2003JD004436>. URL: <https://agupubs.onlinelibrary.wiley.com/doi/abs/10.1029/2003JD004436>.
- Kinne, Stefan et al. (2017). “ESA Climate Change Initiative *aerosolcci2* Product Validation and Intercomparison Report (D4.1b)”. In: URL: http://cci.esa.int/sites/default/files/Aerosol_cci2_PVIR_v3.41.pdf.
- Klüser, Lars (2017). “ESA Climate Change Initiative *aerosolcci2* IMARS Dust properties retrieval Algorithm Theoretical Basis Document (ATBD) Version 2.1”. In: URL: http://cci.esa.int/sites/default/files/Aerosol_cci2_ATBD_IASI_IMARS_v2.0.pdf.
- Klüser, Lars et al. (2016). “Optical properties of non-spherical desert dust particles in the terrestrial infrared – An asymptotic approximation approach”. In:
- Li, Junran et al. (2007). “Quantitative effects of vegetation cover on wind erosion and soil nutrient loss in a desert grassland of southern New Mexico, USA”. In: *Biogeochemistry* 85.3, pp. 317–332. ISSN: 1573-515X. DOI: 10.1007/

- s10533-007-9142-y. URL: <https://doi.org/10.1007/s10533-007-9142-y>.
- Marticorena, Béatrice and Gilles Bergametti (1996). “Two-year simulations of seasonal and interannual changes of the Saharan dust emissions”. In: *Geophysical Research Letters* 23.15, pp. 1921–1924. DOI: 10.1029/96GL01432. eprint: <https://agupubs.onlinelibrary.wiley.com/doi/pdf/10.1029/96GL01432>. URL: <https://agupubs.onlinelibrary.wiley.com/doi/abs/10.1029/96GL01432>.
- Moran-Zuloaga, Daniel et al. (2018). “Long-term study on coarse mode aerosols in the Amazon rain forest with the frequent intrusion of Saharan dust plumes”. In: *Atmospheric Chemistry and Physics* 18, pp. 10055–10088. DOI: 10.5194/acp-18-10055-2018.
- Petzold, ANDREAS et al. (2009). “Saharan dust absorption and refractive index from aircraft-based observations during SAMUM 2006”. In: *Tellus B* 61.1, pp. 118–130. DOI: 10.1111/j.1600-0889.2008.00383.x. eprint: <https://onlinelibrary.wiley.com/doi/pdf/10.1111/j.1600-0889.2008.00383.x>. URL: <https://onlinelibrary.wiley.com/doi/abs/10.1111/j.1600-0889.2008.00383.x>.
- Schwartz, Stephen E. and Meinrat O. Andreae (1996). “Uncertainty in Climate Change Caused by Aerosols”. In: *Science* 272.5265, pp. 1121–1121. ISSN: 0036-8075. DOI: 10.1126/science.272.5265.1121. eprint: <http://science.sciencemag.org/content/272/5265/1121.full.pdf>. URL: <http://science.sciencemag.org/content/272/5265/1121>.
- Slingo, A. et al. (2006). “Observations of the impact of a major Saharan dust storm on the atmospheric radiation balance”. In: *Geophysical Research Letters* 33.24. DOI: 10.1029/2006GL027869. eprint: <https://agupubs.onlinelibrary.wiley.com/doi/pdf/10.1029/2006GL027869>. URL: <https://agupubs.onlinelibrary.wiley.com/doi/abs/10.1029/2006GL027869>.
- Vandenbussche, Sophie (2017). “ESA Climate Change Initiative aerosolcci2 MAPIR Dust properties retrieval Algorithm Theoretical Basis Document (ATBD) Version 2.1”. In: URL: http://cci.esa.int/sites/default/files/Aerosol_cci2_ATBD_IASI_MAPIR_v3.5.pdf.
- Wagner, Frank et al. (2009). “Properties of dust aerosol particles transported to Portugal from the Sahara desert”. In: *Tellus B: Chemical and Physical Meteorology* 61.1, pp. 297–306. DOI: 10.1111/j.1600-0889.2008.00393.x. eprint: <https://doi.org/10.1111/j.1600-0889.2008.00393.x>. URL: <https://doi.org/10.1111/j.1600-0889.2008.00393.x>.